International Journal of Technology 15(4) 1056-1070 (2024)
Received July 2023 / Revised August 2023 / Accepted February 2024

International Journal of Technology

http://ijtech.eng.ui.ac.id

Kinematic and Parametric Modeling of 6DOF(Degree-of-Freedom) Industrial Welding Robot Design and Implementation

Louie Villaverde[1], Dechrit Maneetham[1*]

[1]*Department of Mechatronics Engineering, Rajamangala University of Technology Thanyaburi 39 Moo 1, Khlong 6, Khlong Luang Pathum Thani 12110 Thailand*

Abstract. The increasing demand for automated equipment for precision and versatility requires innovative methods in manufacturing. Despite the high demand, the design and development of industrial robot systems are costly, showing the importance of improving design conceptualization phase. Therefore, this study aimed to address the need by developing an industrial welding robot using a parametric and kinematic modeling method. The investigation focused on the design of six degree of freedom (6DOF) industrial robotic arm for arc welding, exploring kinematic model and dimensional parameters of robotic structure. Computer-aided design (CAD) was applied for modeling and analysis, using Denavit-Hartenberg (DH) convention for mathematical analysis of link and frame movements. This study introduced forward kinematic simulation, which included exploring the position and orientation of the end effector regarding the joint angular values and link parameters. Furthermore, the development of kinematic model of robotic mechanism was proposed to describe the behavior of the physical system compared to an actual robot assembly. Due a reduction ratio of 80 from a rated torque of 22 Nm at a 2000r/min input harmonic drive, the system mechanism was fabricated and assembled. The results showed that robot successfully performed welding process, as indicated by tests carried out using a four-point movement. Moreover, further separate studies should be conducted to assess the quality of welds.

Keywords: Industrial robot design; Kinematic model; Parametric modelling; Robotic simulation

1. Introduction

Industrial robot applications are improving product quality due to their reliability and precision in motion (Xu *et al.*, 2017). This robot is also used in handling toxic or heavy items making a workplace safer. Repetitive tasks for workers are replaced by robot deployed in the manufacturing setup as well as in automating the factory floor (Zeng, Liu, and You, 2019; Fan, Wang, and Xiao, 2014). Currently, industrial factories are searching for cost-effective strategies to enhance the productivity and quality of processes (Krishnan and Sankar, 2022). Among the processes that apply robot in welding (Zeng, Liu, and You, 2019), a fabrication method typically used when combining or joining two different parts (Chen *et al.*, 2016). Specifically, positional accuracy significantly affects welding quality, representing the ability of robot to precisely position the end effector, which handles welding torch to the target points (Baskoro, Kurniawan, and Haikal, 2019).

Consistency in achieving high quality makes robotic welding advantageous to manual

*Corresponding author's email: dechrit_m@rmutt.ac.th, Tel.: +66 (0) 2549 4430
doi: 10.14716/ijtech.v15i4.6559

operation, thereby conferring a competitive edge to industrial applications, particularly automating the process (Wu *et al.*, 2015). Examples of the demand for robotic arc welding are the automotive industry and electronics manufacturing assembly lines(Kah *et al.*, 2015). This robot executes the programmed commands to perform welding operations with minimal human intervention (Dinham and Fang, 2013), although there is a challenge in designing and fabrication. Recently, standard commercial robot has been available for deployment in the industrial setup (Bilancia *et al.*, 2023), leading to the development of the mechanical design of robot in this study. Building an industrial robot requires a significant amount of initial financial investment, as conceptualization plays an essential role in minimizing developmental costs(Wang *et al.*, 2024). Therefore, this study aimed to contribute to the cost-effective and optimal development of custom industrial robot.

Based on the background above, this study focused on designing and assembling robot system for welding applications, considering standard methods (Vasilev *et al.*, 2021). The design of robot for industrial applications starts with the mechanical structure (Zeng, Liu, and You, 2019), which includes the configuration of robot mechanism using kinematic modeling. In this context, the configuration of six degree of freedom (6DOF) robotic manipulator is suitable for industrial processes such as welding. Therefore, the analysis of the movement of end effector position and orientation is based on the rigid component's measurements and joint angle (Nektarios and Aspragathos, 2010). The custom mechanical design of robot also contributes to the concept of industrial modularity and ease of fabrication. The development process is carried out to construct a parametric model of the industrial welding robot including the parameters' topology (Zhang *et al.*, 2022). To optimize the movement or rigidity characteristics, adjustment was made to these parameters, and selection was based on the dimensions conceived from the developed kinematic model(Russo *et al.*, 2024). This study also applied a paradigm shift in the optimization of robot characteristics through the derivation of parameters using the developed kinematic model and simulation.

Several studies have been conducted on design of industrial robot. For example, (Li and Wang, 2019) used genetic algorithm for optimization, while (Jiang *et al.*, 2020) focused on accuracy improvement using artificial networks by algorithm with differential evolution. Furthermore, there is a study on selecting industrial robot used for arc welding (Chodha *et al.*, 2021) through the implementation and presentation of simulated and actual experimental results. According to (Pramujati *et al.*, 2023), parallel robot modeling based on a control position of cable-driven servo motors was proposed for design mechanism and system development using existing literature.

This study is significantly different from previous investigations by including comprehensive kinematic and parametric modeling in the development of industrial robot. Conceptualization of new hardware components for industrial robot application is simplified using simulated models. The use of computer system can help save the cost associated with the building process. Moreover, modeling kinematic before developing robot control is significant, as these models are categorized as forward and inverse kinematic (Farzan and Desouza, 2013). The pose is described using a set matrix or vectors in Cartesian coordinate system, with kinematic model having constraints such as joint angle, link length, inertia, etc(Andersen, 2020). The joint variables measured in angles for each link directly reflect end effector pose (Pham *et al.*, 2018). The challenge of this study is to design the dimensions and physical components of each link based on analysis of kinematic model described using lengths and Denavit-Hartenberg (DH) convention.

In this study, kinematic model leading to the physical structure is presented using the software. Establishing a conceptual kinematic model is important to design the desired

motion of robotic system (Fazel, Shafei, and Nekoo, 2024). After the analysis, the physical structure of the system is designed to match the specifications of kinematic model. By defining the motion of robotic arm system through kinematic model, the physical structure could be developed effectively and optimized by iterative processes. This model is specifically subjected to forward kinematic and robot is modeled for simulation, guiding the actual design and implementation. Moreover, the physical systems are modeled using CAD software, and the control can be simulated with MATLAB Robotics Toolbox for validation (Crenganis *et al.*, 2019; Liu, Liu, and Tian, 2019). Robot can be modeled as a kinematic chain according to the mechanical structure, showing the dimension and structure of robotic arm for kinematic modelling (Singh and Singla, 2017).

The contributions made in this study included (1) the effect of kinematic on the position of welding torch. (2) A new industrial welding robot design based on revolute joint was fabricated and assembled along with essential parts including links and servo motors, as a custom-made welding robot developed first in Thailand. Changing the joint angles of each axis affected the position and orientation of the end-effector, namely welding torch. This was because the integration of robotic components from a design in Thailand to fit an industrial application such as welding was considered more economical.

This study was organized as follows, Section 2 discussed methods of the mechanical structure, kinematic model, and forward kinematic model. Section 3 presented the results and discussion, while Section 4 concluded this study and presented future endeavors.

2. Methods

2.1. Mechanical Structure

The criteria for designing a custom-made robotic arm were established by considering a serial robot configuration and range of motion to determine the dimensions of each link. Industrial robot joints could be prismatic or revolute, depending on the application. In this study, the configuration of joints is all revolute, which was in line with the common standard of industrial welding. The anthropomorphic structure was composed of the waist, shoulders, elbows, also wrists, which corresponded to the joints of the human arm (Megalingam *et al.*, 2018), as shown in Figure 1. Moreover, Figure 2 shows the mechanism of robotic arm, where the wrist articulates in three directions (yaw, roll, pitch), which increases the ability of the end effector to become flexible when manipulating welding tool. The parameters of the design mechanism are presented in Table 1, which includes Range of Motion (ROM), while the Link lengths and offsets are shown in Table 2. The range of motion is designed for parameters pitch, yaw, roll, waist, shoulder, and elbow, considering cabling and inertia. The link lengths were based on the potential reach of robot. Additionally, the digital prototype was made using 3D tool to develop the physical systems model, which showed the dimensions, weight, appearance, and other characteristics of robot arm.

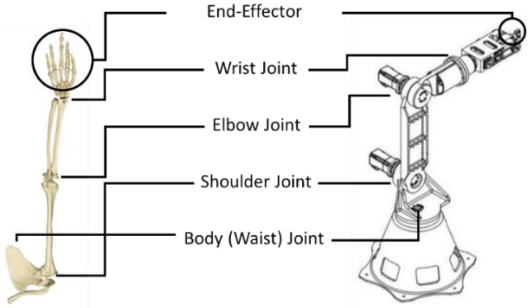

Figure 1 Anthropomorphic Arm Configuration

Table 1 Robotic Arm Specification

Feature	Description
Range of Motion (ROM)	Wrist - Pitch: 180°, Roll:180°, Yaw:180°, Elbow: 130°, Shoulder: 110°, Waist: 180°

Table 2 Link Lengths and Offsets

Joint	Waist	Shoulder	Elbow	Wrist
Symbol	L1	L2	L3	L4
Link Length (mm)	635	650	455	421

2.2. Forward Kinematic (FK)

Forward kinematic is the study of describing the position and orientation of the end effector in terms of the joint angular values and link parameters (Vacharakornrawut *et al.*, 2016; Mehmood *et al.*, 2014). This can be solved by determining the homogeneous transformation matrix through the combination of the rotational matrix and the displacement vector. Moreover, the mathematical solution of forward kinematic is based on DH parameters (Bian, Ye, and Mu, 2016). The convention is a maturely recognized parameterization for industrial robot modelling (Zhao *et al.*, 2018), which is carried out by computing the product of the homogeneous matrices resulting in the final transformation matrix (Ritboon and Maneetham, 2019). The product is used to identify the pose of the end effector, given the joint parameters, in the form of Special Euclidean (SE) (3) or 4x4 homogeneous matrix composed of the rotation matrix and displacement vector. The initial step in determining forward kinematic of the manipulator is categorizing each frame using DH parameters (Bouzgou and Ahmed-Foitih, 2014), which is called kinematic model as shown in Figure 3. The construction of kinematic model follows the right-hand rule and DH parameters can be found based on the frame assignment, as shown in Table 3. Each column is assigned for specified parameters, named joint angle (θ), angle of twist (α), link offset (d), and link length (a). This is carried out to precisely determine the spatial configuration of robotic arm by establishing kinematic model and applying forward kinematic simulation, thereby contributing to the prototyping process of 6DOF robotic arm (Ekrem and Aksoy, 2023).

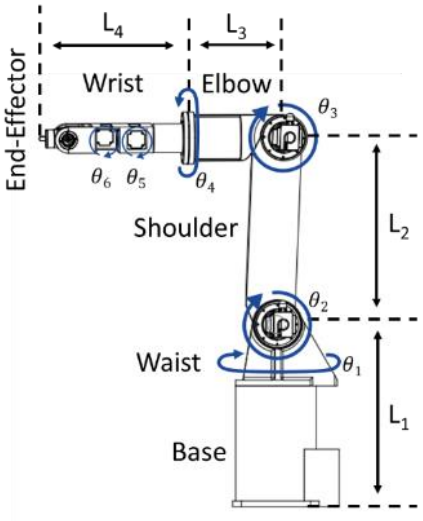

Figure 2 Robotic Arm Configuration showing major mechanical components and direction of articulation

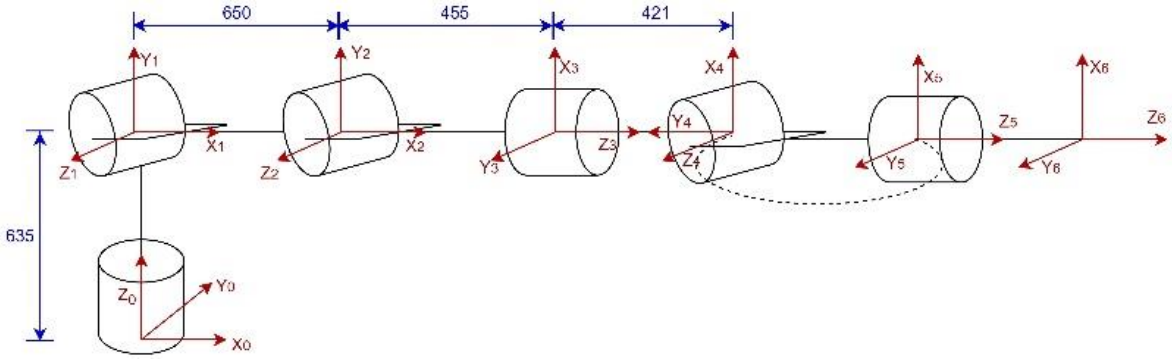

Figure 3 Kinematic Model of the Robotic Arm with dimension

Table 3 DH Parameter

Joint	Joint Angle ($\boldsymbol{\theta}$)	Angle of twist ($\boldsymbol{\alpha}$)	Link Offset (d)	Link Length (a)
1	$\theta 1$	90	635	0
2	$\theta 2$	0	0	650
3	$\theta 3$+90	90	0	455
4	$\theta 4$	-90	421	0
5	$\theta 5$	90	0	0
6	$\theta 6$	0	0	0

Equation 1 shows the general formula of the transformation matrix, T_i^{i-1}. Components of this matrix are dependent on the variables from DH parameter table. The result describes rotation matrix and displacement vector of a coordinate frame based on the adjacent frame.

$$T_i^{i-1} = \begin{bmatrix} \cos\theta_i & -\sin\theta_i\cos\alpha_i & \sin\theta_i\sin\alpha_i & a_i\cos\theta_i \\ \sin\theta_i & \cos\theta_i\cos\alpha_i & -\cos\theta_i\sin\alpha_i & a_i\sin\theta_i \\ 0 & \sin\alpha_i & \cos\alpha_i & d_i \\ 0 & 0 & 0 & 1 \end{bmatrix} \quad (1)$$

The general formula was applied to respective components from DH parameter table. The substitution of the values corresponding to respective joint and link parameters led to individual transformation matrix per coordinate frame. Simulation and modeling were made to validate the equation and analyze kinematic of robot arm using MATLAB software.

$$T_1^0 = \begin{bmatrix} \cos\theta_1 & -\sin\theta_1\cos\alpha_1 & \sin\theta_1\sin\alpha_1 & a_1\cos\theta_1 \\ \sin\theta_1 & \cos\theta_1\cos\alpha_1 & -\cos\theta_1\sin\alpha_1 & a_1\sin\theta_1 \\ 0 & \sin\alpha_1 & \cos\alpha_1 & d_1 \\ 0 & 0 & 0 & 1 \end{bmatrix} \quad (2)$$

$$T_2^1 = \begin{bmatrix} \cos\theta_2 & -\sin\theta_2 & 0 & 650\cos(\theta_2) \\ \sin\theta_2 & -\cos\theta_2 & 0 & 650\sin(\theta_2) \\ 0 & 0 & 1 & 0 \\ 0 & 0 & 0 & 1 \end{bmatrix} \quad (3)$$

$$T_3^2 = \begin{bmatrix} \cos\theta_3 & -\sin\theta_3 & \sin\theta_3 & 455\cos(\theta_3) \\ \sin\theta_3 & -\cos\theta_3 & -\cos\theta_3 & 455\sin(\theta_2) \\ 0 & 1 & 0 & 0 \\ 0 & 0 & 0 & 1 \end{bmatrix} \quad (4)$$

$$T_5^4 = \begin{bmatrix} \cos\theta_5 & -\sin\theta_5 & \sin\theta_5 & 0 \\ \sin\theta_5 & -\cos\theta_5 & -\cos\theta_5 & 0 \\ 0 & 1 & 0 & 0 \\ 0 & 0 & 0 & 1 \end{bmatrix} \quad (5)$$

$$T_5^4 = \begin{bmatrix} \cos\theta_5 & -\sin\theta_5 & \sin\theta_5 & 0 \\ \sin\theta_5 & -\cos\theta_5 & -\cos\theta_5 & 0 \\ 0 & 1 & 0 & 0 \\ 0 & 0 & 0 & 1 \end{bmatrix} \quad (6)$$

$$T_6^5 = \begin{bmatrix} \cos\theta_6 & -\sin\theta_6 & 0 & 0 \\ \sin\theta_6 & \cos\theta_6 & 0 & 0 \\ 0 & 0 & 1 & 0 \\ 0 & 0 & 0 & 1 \end{bmatrix} \quad (7)$$

Equations 2-7 are substitutions of the values each respective frame. The application of the equation to 6DOF robotic arm manipulator includes the multiplication for respective transformation matrix. The result is reflected in matrix T_6^0 from the base to the end effector frame. Equation 8 shows the final transformation matrix as a product of all transformation matrices with respect to the frame assignment.

$$T_6^0 = T_1^0 T_2^1 T_3^2 T_4^3 T_5^4 T_6^5 \quad (8)$$

2.3. Post Processor

The tasks of the system for translating the joint angles to the specific tool location were designed in the post processor stage. In this section, the mechanism of transformation was discussed. Initially, the post processor of robotic arm was developed using Programmable Logic Control (PLC), with servo motors executed through drivers as the final actuating elements. The ladder logic design focused on transmitting signal from GUI, which showed the joint angle of the axis, along with the tool position. To ensure the program executed the intended position and orientation, ROM was considered along with workspace requirements and coordinate system relating to the physical world. Calibration of each axis joint angle with the servo motor was carried out by checking the angle against the corresponding feedback from drivers' encoders. Simulating each corresponding angle by jogging axis using robot pendant was performed to verify the response of the servo motor driver and motors. Subsequently, data collection was carried out by recording the angles versus input feedback from the servo motors' absolute encoder.

3. Results and Discussion

3.1. Forward Kinematic Simulation

Kinematic simulation model was performed using MATLAB Robotics Toolbox. The numerical results, combined with a visual plot of robot's pose in MATLAB software, provide a comprehensive knowledge of the end effector pose. The results have been plotted using various joint angles as inputs to the forward kinematic model and MATLAB Robotics Toolbox. Subsequently, visual simulation is performed by feeding the four parameters derived from the six links using the software.

The process is carried out with several different joint configuration value scenarios. The first scenario, [0 0 0 0 0 0] results in the position of the xyz end effector at [421 0 1740] with a yaw, pitch, and roll of [0 90 180]. This is followed by matrix value generated using

the first scenario, while the results of robot arm simulation plot are shown in Figure 4 and Equation 9.

$$ {}^{0}_{6}T = \begin{bmatrix} 0 & 0 & 1 & 421 \\ 0 & -1 & 0 & 0.00 \\ 1 & 0 & 0 & 1740 \\ 0 & 0 & 0 & 1 \end{bmatrix} \tag{9} $$

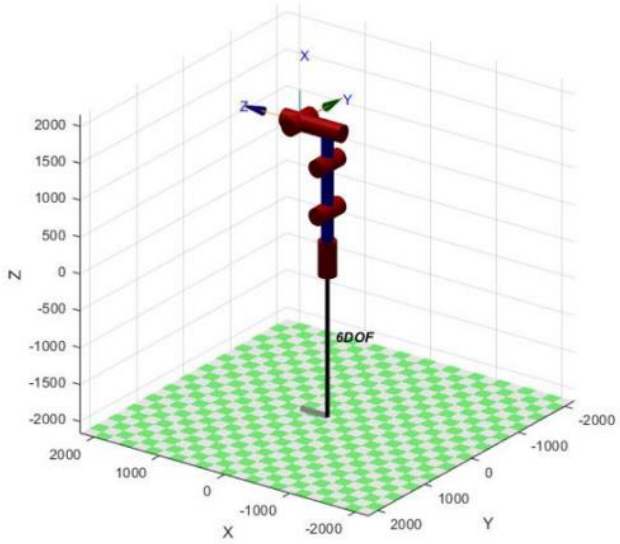

Figure 4 Visualization from Plot function for [0 0 0 0 0 0] configuration

The second scenario with the value of the joint angle configuration is set to [-15 -15 -15 0 0 0], followed by the xyz end effector position [734 -196.8 1446.39] and the yaw pitch roll end effector value [28.2 56.8 155.9], as shown in Figure 5 and Equation 10. Subsequently, matrix and simulation plots are obtained from scenario.

$$ {}^{0}_{6}T = \begin{bmatrix} 0.4830 & -0.2588 & 0.8365 & 734.4 \\ -0.1294 & -0.9659 & -0.2241 & -196.8 \\ 0.8660 & 0 & -0.5000 & 1446.39 \\ 0 & 0 & 0 & 1 \end{bmatrix} \tag{10} $$

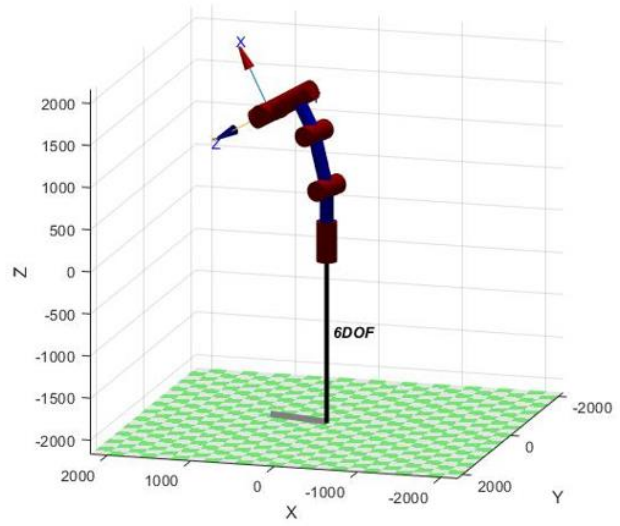

Figure 5 Visualization from Plot function for [-15 -15 -15 0 0 0] configuration

In the third scenario, the joint angle configuration is set to [-30 -30 -30 0 0 0], resulting in the position of the xyz end effector [805 -464.8 1061], with a roll value of yaw, pitch, and roll value of [33.7 25.7 163.9]. The results of the calculation of the third scenario matrix are shown in Figure 6 and Equation 11.

$$ {}^{0}_{6}T = \begin{bmatrix} 0.7500 & -0.5000 & 0.4330 & 805 \\ -0.4330 & -0.8660 & -0.2500 & -464.8 \\ 0.5000 & 0 & -0.8660 & 1061 \\ 0 & 0 & 0 & 1 \end{bmatrix} \quad (11) $$

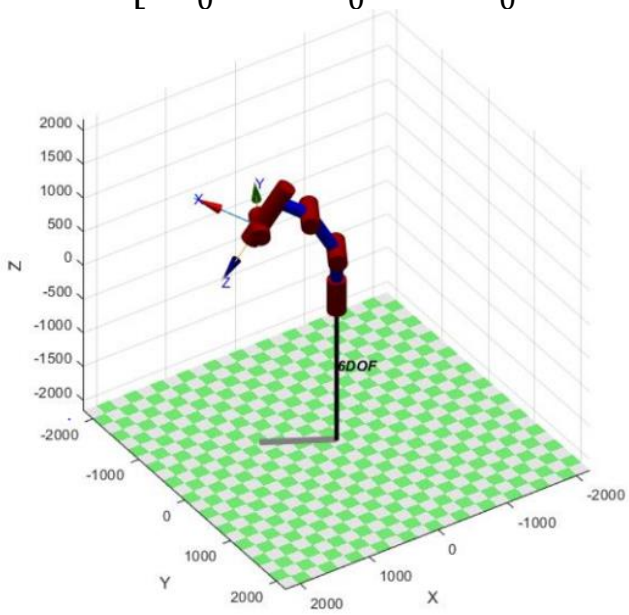

Figure 6 Visualization from Plot function for [-30 -30 -30 0 0 0] configuration

Forward kinematic is an essential requirement in building industrial robot to establish the relationship between the joint angle and tool position. Furthermore, it serves as a fundamental theory during the development of robotic arm, particularly when the application does not require autonomous control. In this study, MATLAB was used for simulation and analysis (Junior *et al.*, 2011).

3.2. Parametric Modeling

This study is divided into two stages, namely design and implementation. CAD software is used during the design stage to create 3D models (Kholil *et al.*, 2023), which is critical due to the potential for cost-efficient implementation. The second stage is the implementation, where the process of constructing CAD design using various materials is initiated. Certain components of robot are made of aluminum, while others are cast alloy steel. The 2D models shown in Figures 7, 8, and 9 are based on the arbitrary links made from kinematic model.

One of the contributions of this study is a novel design of 6 DOF industrial robotic arm, presented in Figure 7, as 2D parametric model of (a) elbow link (b) wrist link, and (c) shoulder link. Figures 8 (a), (c), (e), (g), (i), and (k) are the results of 3D model design using CAD application, while (b), (d), (f), (h), (j), and (l) are the actual robot implementation. The total weight of the mechanism including the motors is 155 kilograms. There is an application of the harmonic gear concept in Figures 8 (i) and (j), while Figures 8 (k) and (l) are the design of the end effector link model to enable movement in roll and pitch. Moreover, the system has a reduction ratio of 80 from a rated torque of 22 Nm with a 2000r/min input.

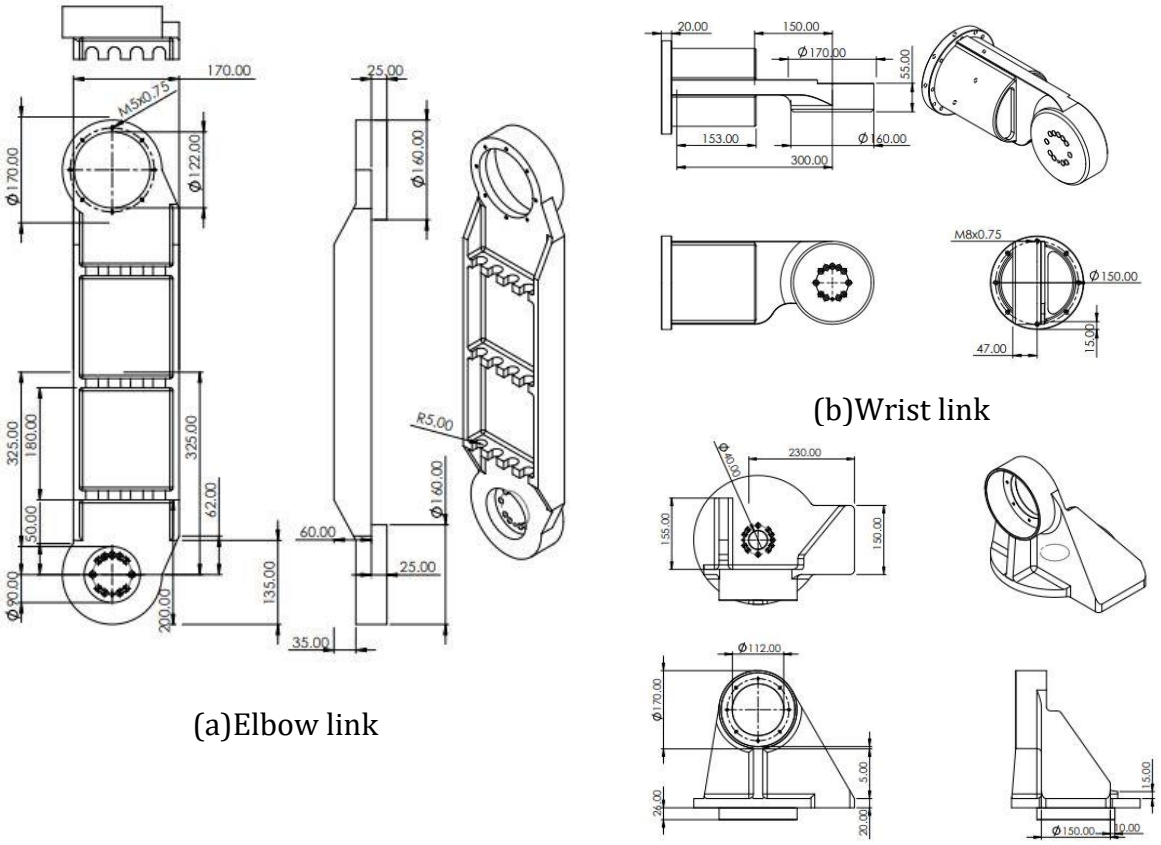

(a)Elbow link

(b)Wrist link

(c)Shoulder link

Figure 7 2D Parametric model. Components labeled as (a) Elbow link, (b) Wrist link, (c) Shoulder link

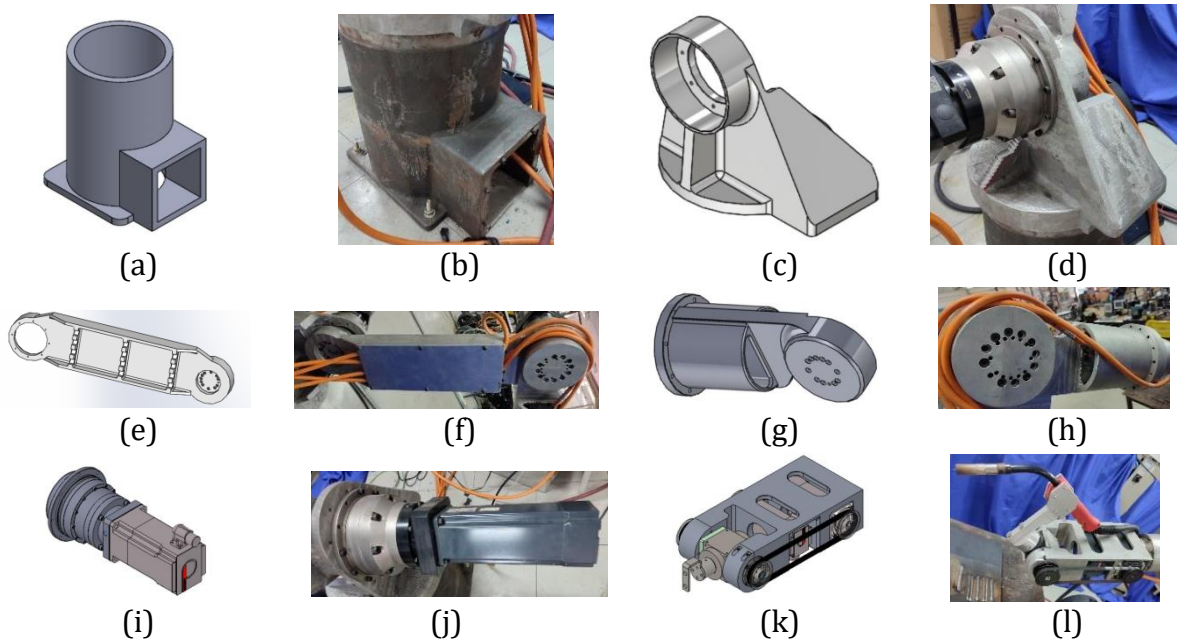

(a) (b) (c) (d)

(e) (f) (g) (h)

(i) (j) (k) (l)

Figure 8 3D model and Actual. These images are components, which are labeled as (a)Base Model, (b) Actual Base, (c)Shoulder Link Model, (d) Actual Shoulder Link, (e) Elbow Link Model, (f) Actual Elbow Link, (g) Wrist Link, Model (h) Actual Wrist Link, (i) Servo Motor and Harmonic Gear Model, (j) Actual Servo Motor and Harmonic Gear, (k) End Effector Link Model, (l) Actual End-Effector Link

3.3. Implementation

Figure 9 shows the schematics and control box, which consists of six servo motors connected to three servo drives, with robot's CPU being a Beckhoff C5102-0040. Additionally, the Ehave-CM350 serves as welding machine that is connected to the IO Device through USB cable for remote control. The arm is fully driven with each DOF achieved by a precision servo motor equipped with a three-phase synchronous motor excited by a permanent magnet. The specifications of the servo motor used are shown in Table 4.

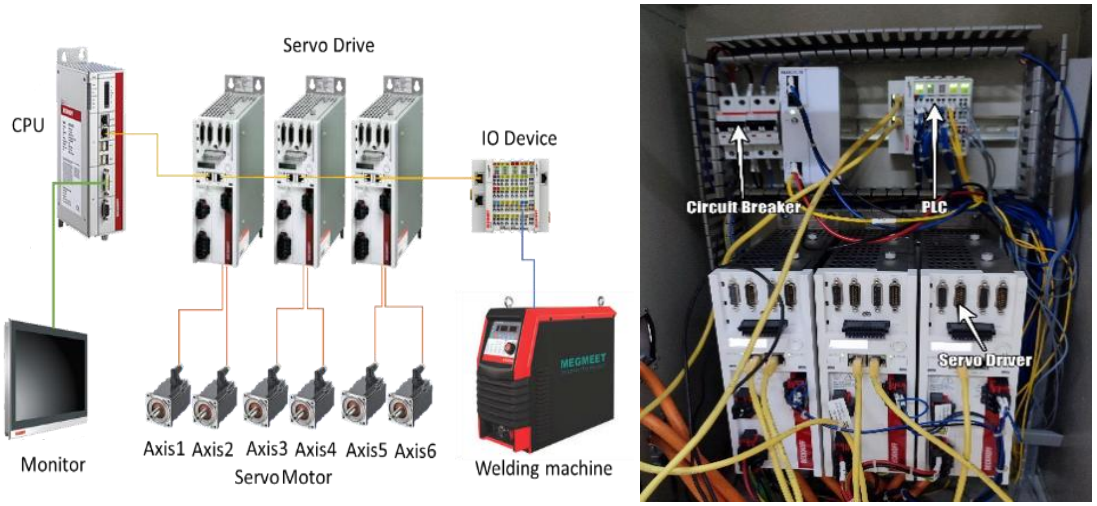

(a) (b)

Figure 9 Schematics of the Control Box: (a) schematics, (b) actual devices

Table 4 Servo Motor Specification

Specification	Servo 1	Servo 2
Motor type	AM8023-wEyz	AM8043-wHyz
Nominal voltage	100…480 V AC	100…480 V AC
Standstill torque	1.20 Nm	5.65 Nm
Rated torque	1.00 Nm	4.90 Nm
Peak torque	6.36 Nm	28.0 Nm
Rated speed	8000 min-1	5000 min-1
Rated power	0.84 kW	2.57 kW
Standstill current	2.20 A	5.40 A
Peak current	11.40 A	31.0 A
Torque constant	0.54 Nm/A	1.04 Nm/A
Rotor moment of inertia	0.378 kgcm^2	kgcm^2

This study uses 6DOF robotic arm manipulator developed using Beckhoff PLC with TWINCAT 3 software and CPU is a Beckhoff C5102-0040. MEGMEET Ehave-CM350 is used as welding machine that is connected to IO Device through a serial communication cable for remote control. The actual assembly is presented in Figure 10, showing the implementation of the parametric and kinematic modeling.

The developed system is subjected to the same values from simulation. The joint angle parameters are set in degrees, consistent with the values from MATLAB simulations. Comparing the visualization of the simulated and actual values validates the similarity in terms of the configurations. Positional accuracy was obtained by comparing robotic position and the simulation, as presented in Figure 11. The actual position of robot was conducted using GUI designed to locate the angles of each axis according to the user's input.

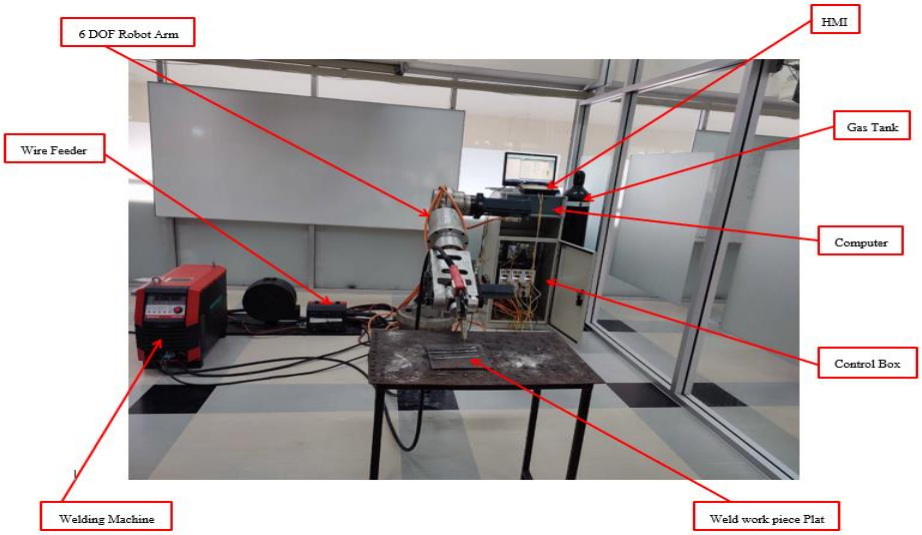

Figure 10 Actual Assembly of Welding Robot

Robot arm was subjected to implement welding process shown in Figure 12. The feedback from the servo motors corresponding to each axis was analyzed by comparing the numerical value against angle to assess the accuracy of robot. The results shown in Figure 13 represent the actual collected data related to robot's accuracy characterized by the input angle. Since the motion is controlled by a pendant graphical user interface, the collected data corresponded only with feedback from servo motors drive, as measured using the Beckhoff software. The process includes position control of welding torch towards the plate to be tested. The four-point pose of the industrial robot was recorded and position graphs were drawn in Figure 13. Subsequently, robot performed a linear motion to assess welding accuracy.

Figure 13 shows the position graph regarding the four-point movement of each axis of robot. The vertical axis shows the time value in minutes and the horizontal axis represents angles programmed for welding process. The graph was generated from the sensors value from Beckhoff software TwinCAT 3 versus the angle user intends to locate the end effector of robot.

(a) (b) (c)

Figure 11 Actual Robot Position (a) [0,0,0,0,0,0], (b) [-15,-15,-15,0,0,0], (c) [-30,-30,-30,0,0,0]

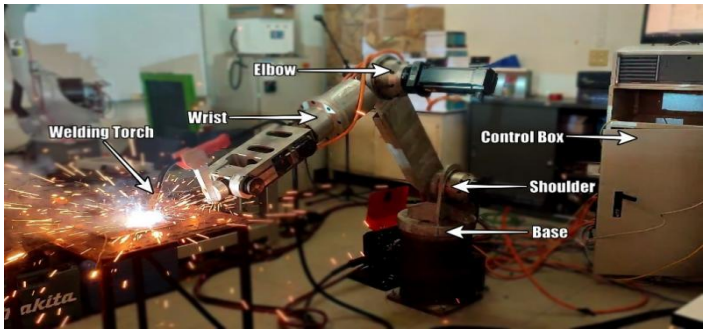

Figure 12 Actual Welding Process

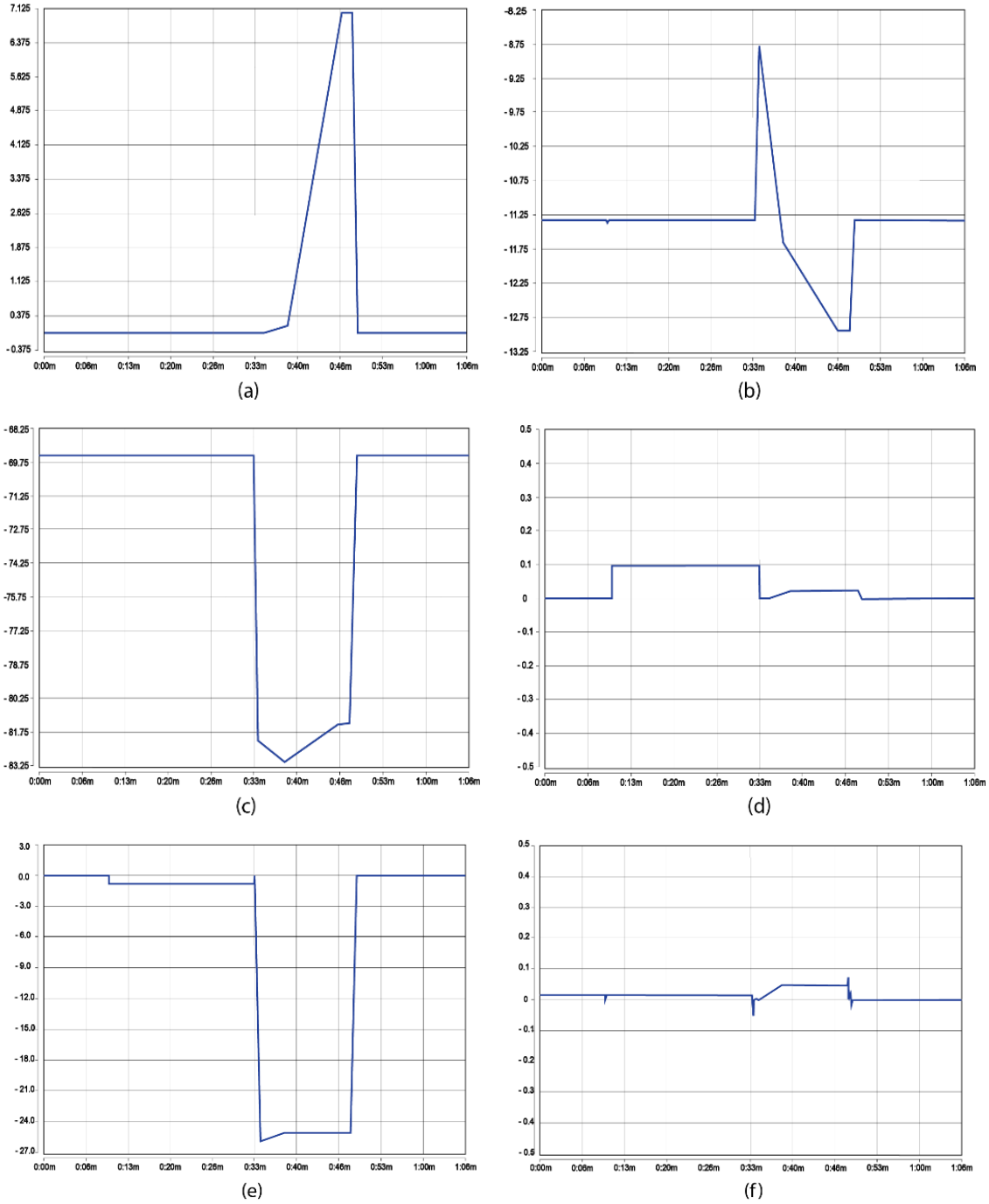

Figure 13 Position Graphs (a) Joint Axis 1, (b) Joint Axis 2, (c) Joint Axis 3, (d) Joint Axis 4, (e) Joint Axis 5, (f) Joint Axis 6

4. Conclusions

In conclusion, this study successfully developed 6DOF industrial robotic arm for metal arc welding, along with the structure. The description and analysis of kinematic model were obtained using right hand rule. Forward kinematic was solved using the resultant of the final transformation matrix from DH parameter. Mechanical structure was drawn in the feature-based, parametric modeling software SolidWorks. Actual implementation of robot was also tested with the joints measured at four-point in the workspace. An industrial robotic articulated jointed arm was designed and built along with the structure, with modeling kinematic serving as the fundamental step before developing parametric design. Robot was simulated in three different positions with angles and kinematic model was performed using MATLAB Robotics Toolbox. The manipulator was fabricated and assembled, showing a reduction ratio of 80 from a rated torque of 22 Nm from a 2000r/min input. Welding process was arc welding with the butt-weld method implemented for robot functionality. Therefore, further studies were recommended for the quality of welds.

Acknowledgments

The authors are grateful to colleagues from the Doctor of Engineering for diligently helping us write the draft of the study in terms of graphic designs. Furthermore, the authors are grateful to the Department of Mechatronics Engineering, Faculty of Technical Education, for the academic support which contributed to the successful completion of this study.

References

Andersen, M.S., 2020. Introduction to musculoskeletal modelling. *In Computational Modelling of Biomechanics and Biotribology in the Musculoskeletal System: Biomaterials and Tissues.* Elsevier, pp. 41–80

Baskoro, A.S., Kurniawan, R.P., Haikal, 2019. Evaluation of the 2-Axis Movement of a 5-Axis Gantry Robot for Welding Applications. *International Journal of Technology,* Volume 10(5), pp. 1024–1032

Bian, Z., Ye, Z., Mu, W., 2016. Kinematic Analysis and Simulation of 6-DOF Industrial Robot Capable of Picking up Die-Casting Products. *In*: AUS 2016 - 2016 IEEE/CSAA International Conference on Aircraft Utility Systems, pp. 41–44

Bilancia, P., Schmidt, J., Raffaeli, R., Peruzzini, M., Pellicciari, M., 2023. An Overview of Industrial Robots Control and Programming Approaches. *Applied Sciences*, Volume 13(4), p. 2582

Bouzgou, K., Ahmed-Foitih, Z., 2014. Geometric Modeling and Singularity of 6 DOF Fanuc 200IC Robot. *In* 4th International Conference on Innovative Computing Technology, INTECH 2014 and 3rd International Conference on Future Generation Communication Technologies, FGCT 2014, pp. 208–214

Chen, K., Cao, G., Sun, J., Yang, J., 2016. A Path-Planning Algorithm of The Automatic Welding Robot System for Three-Dimensional Arc Welding Using Image Processing. *In:* 2016 13th International Conference on Ubiquitous Robots and Ambient Intelligence, URAI 2016, pp. 692–697

Chodha, V., Dubey, R., Kumar, R., Singh, S., Kaur, S., 2021. Selection of Industrial Arc Welding Robot with TOPSIS and Entropy MCDM Techniques. *In:* Materials Today: Proceedings. Elsevier Ltd, pp. 709–715

Crenganis, M., Tera, M., Biris, C., Gîrjob, C., 2019. Dynamic Analysis of a 7 DOF Robot Using Fuzzy Logic for Inverse Kinematics Problem. *Procedia Computer Science,* Volume 162, pp. 298–306

Dinham, M., Fang, G., 2013. Autonomous Weld Seam Identification and Localisation Using Eye-In-Hand Stereo Vision for Robotic Arc Welding. *Robotics and Computer-Integrated Manufacturing,* Volume 29(5), pp. 288–301

Ekrem, Ö., Aksoy, B., 2023. Trajectory Planning for A 6-Axis Robotic Arm with Particle Swarm Optimization Algorithm. *Engineering Applications of Artificial Intelligence*, Volume 122, p. 106099

Fan, X., Wang, X., Xiao, Y., 2014. A Combined 2D-3D Vision System for Automatic Robot Picking*. In:* International Conference on Advanced Mechatronic Systems, pp. 513–516

Farzan, S., Desouza, G.N., 2013. From D-H to Inverse Kinematics: A Fast Numerical Solution for General Robotic Manipulators Using Parallel Processing. *In:* IEEE International Conference on Intelligent Robots and Systems, pp. 2507–2513

Fazel, R., Shafei, A.M., Nekoo, S.R., 2024. Dynamic Modeling and Closed-Loop Control Design for Humanoid Robotic Systems: Gibbs–Appell Formulation and SDRE Approach. In *Multibody System Dynamics*

Jiang, Y., Yu, L., Jia, H., Zhao, H., Xia, H., 2020. Absolute Positioning Accuracy Improvement in an Industrial Robot, Sensors, Volume 20(16), p. 4354

Junior, J., Marcos, R., Tenório, C., Mateus, A., Egoavil, C., 2011. Development of a Matlab Software for Real-time Mapping of Electric Fields on Transmission Power Line. *International Journal of Technology,* Volume 2, pp. 164–170

Kah, P., Shrestha, M., Hiltunen, E., Martikainen, J., 2015. Robotic Arc Welding Sensors and Programming in Industrial Applications. *International Journal of Mechanical and Materials Engineering*, Volume 10(13), pp. 1–16

Kholil, A., Kiswanto, G., Al Farisi, A., Istiyanto, J., 2023. Finite Element Analysis of Lattice Structure Model with Control Volume Manufactured Using Additive Manufacturing. *International Journal of Technology,* Volume 14(7), pp. 1428–1437

Krishnan, M.G., Sankar, A., 2022. Image Space Trajectory Tracking of 6-DOF Robot Manipulator in Assisting Visual Servoing. Automatika, Volume 63(2), pp. 199–215

Li, G., Wang, Y., 2019. Industrial Robot Optimal Time Trajectory Planning Based on Genetic Algorithm. *In:* Proceedings of 2019 IEEE International Conference on Mechatronics and Automation, ICMA 2019, pp. 136–140

Liu, Y., Liu, Y., Tian, X., 2019. Trajectory and Velocity Planning of The Robot for Sphere-Pipe Intersection Hole Cutting with Single-Y Welding Groove. Robotics and Computer-Integrated Manufacturing, Volume 56, pp. 244–253

Megalingam, R.K., Katta, N., Geesala, R., Yadav, P.K., Rangaiah, R.C., 2018. Keyboard-Based Control and Simulation of 6-DOF Robotic Arm using ROS. *In:* 2018 4th International Conference on Computing Communication and Automation, ICCCA 2018, pp. 2–6

Mehmood, N., Ijaz, F., Murtaza, Z., Shah, S., 2014. Analysis of End-Effector Position and Orientation for 2P-3R Planer Pneumatic Robotic Arm. *In:* 2014 International Conference on Robotics and Emerging Allied Technologies in Engineering, iCREATE 2014 Proceedings, pp. 47–50

Nektarios, A., Aspragathos, N.A., 2010. Optimal Location of a General Position and Orientation End-Effector's Path Relative to Manipulator's Base, Considering Velocity Performance. *Robotics and Computer-Integrated Manufacturing*, Volume 26(2), pp. 162–173

Pham, H.L., Adorno, B.V., Perdereau, V., Fraisse, P., 2018. Set-Point Control of Robot End-Effector Pose Using Dual Quaternion Feedback. *Robotics and Computer-Integrated Manufacturing*, Volume 52, pp. 100–110

Pramujati, B., Syamlan, A.T., Nurahmi, L., Tamara, M.N., 2023. Study on the Application of Model-based Control Algorithm for a Suspended Cable-Driven Parallel Robot. *International Journal of Technology,* Volume 14(4), pp. 854–866

Ritboon, V., Maneetham, D., 2019. A New Industrial Robotics and Software Development Resolved the Position and The Speed Control. *In:* 2019 International Conference on Information and Communications Technology, ICOIACT 2019, pp. 674–677

Russo, M., Zhang, D., Liu, X.J., Xie, Z., 2024. A Review of Parallel Kinematic Machine Tools: Design, Modeling, and Applications. *International Journal of Machine Tools and Manufacture*, Volume 196, p. 104118

Singh, A., Singla, A., 2017. Kinematic Modeling of Robotic Manipulators. *In:* Proceedings of the National Academy of Sciences India Section A - Physical Sciences, Volume 87(3), pp. 303–319

Vacharakornrawut, N., Themanee, T., Rerkratn, A., Pongswatd, S., 2016. Converting TCP to Joints Value of 6-DOF Robot Based on Forward and Inverse Kinematic Analysis. *In*: 2016 13th International Conference on Electrical Engineering/Electronics, Computer, Telecommunications and Information Technology, ECTI-CON 2016, pp. 1–6

Vasilev, M., Macleod, C.N., Loukas, C., Javadi, Y., Vithanage, R.K.W., Lines, D., Mohseni, E., Pierce, S.G., Gachagan, A., 2021. Sensor-Enabled Multi-Robot System for Automated Welding and In-Process Ultrasonic Nde. *Sensors,* Volume 21(15), p. 5077

Wang, L., Peng, G., Yang, Y., Li, X., 2024. Industrial Robot Application and Enterprise Financialization: Empirical Evidence from the Chinese Manufacturing Firm Level. *Journal of the Knowledge Economy,* Volume 2024, pp. 1–25

Wu, Y., Ming Go, J.Z., Ahmed, S.M., Lu, W., Chew, C., Pang, C.K., 2015. Automated Bead Layout Methodology for Robotic Multi-Pass Welding. *In:* IEEE International Conference on Emerging Technologies and Factory Automation, pp. 19–22

Xu, Y., Fang, Gu., Du, S., Zhao, W., Ye, Z., Chen, S., 2017. Welding Seam Tracking in Robotic Gas Metal Arc Welding. *Journal of Materials Processing Technology,* Volume 248, pp. 18–30

Zeng, T., Liu, P., You, D., 2019. Kinematics Simulation and Operation Space Analysis of Arc Welding Six-Axis Robot Based on Matlab and Adams. *In:* Proceedings - 2019 2nd World Conference on Mechanical Engineering and Intelligent Manufacturing, WCMEIM 2019, pp. 504–507

Zhang, Y., Xiao, J., Zhang, Z., Dong, H., 2022. Intelligent Design of Robotic Welding Process Parameters Using Learning-Based Methods. *IEEE Access,* Volume 10, pp. 13442–13450

Zhao, R., Shi, Z., Guan, Y., Shao, Z., Zhang, Q., Wang, G., 2018. Inverse Kinematic Solution of 6R Robot Manipulators Based on Screw Theory and The Paden–Kahan Subproblem. *International Journal of Advanced Robotic Systems,* Volume 15(6), pp. 1–11